^{206}Pb(α,d)^{208}Bi at 48 MeV

M. J. Spisak* and W. W. Daehnick
Nuclear Physics Laboratory, University of Pittsburgh, Pittsburgh, Pennsylvania 15260
(Received 23 December 1983)

The ^{206}Pb(α,d)^{208}Bi reaction was investigated at 48.2 MeV with about 25 keV resolution. Angular distributions were obtained for 48 levels at excitation energies up to 5 MeV. Many previously unknown levels were seen and most seem to have two-particle—two-hole structure and spins above 6; however, the relatively structureless angular distributions permit only approximate L assignments. Transitions to six low-lying one-particle—one-hole states were analyzed in detail. Distorted-wave Born approximation predictions agreed with the observed angular distributions, but the absolute cross sections computed from published ^{206}Pb and ^{208}Bi wave functions are generally larger than observed, particularly those for the J_{max} states. Contributions of the dominant two-step sequential stripping channels to the one-step results were investigated. They were important and gave varying amounts of enhancement for all six levels. The observed quenching of the J_{max} cross sections was not reproduced.

I. INTRODUCTION

The low-lying levels of ^{208}Bi are generally interpreted as multiplets resulting from the coupling of a proton particle and a neutron hole outside the $J^{\pi}=0^{+}$, ^{208}Pb core.[1-6] Above approximately 2.5 MeV excitation energy the level structure is expected to become more complicated due to couplings to the core excited states of ^{208}Pb. Kim and Rasmussen,[2] Kuo,[1] and Ma and True[3] have performed detailed shell-model calculations for ^{208}Bi. Their results predict that, in general, the residual interactions will cause only weak configuration mixing for the low-lying states of ^{208}Bi. Single-particle pickup experiments[4-6] have indicated that many ^{208}Bi levels below 3 MeV excitation are in fact of relatively pure configuration. Spectroscopic factors obtained in these experiments generally agree with theoretical calculations, which assume that in ^{208}Bi only one neutron hole and one proton particle are active.

In a previous paper,[7] we reported two-nucleon transfers to some higher lying ^{208}Bi levels which are difficult to excite in single-nucleon transfer reactions. It was found that the ^{208}Bi levels very strongly excited with the ^{206}Pb(α,d)^{208}Bi reaction are two-particle—two-hole J_{max} states. In this paper more comprehensive results for ^{208}Bi will be given. In addition, results of detailed distorted wave Born approximation (DWBA) and coupled channels calculations for six low-lying levels in ^{208}Bi will be given in order to determine if the previously reported[8,9] contributions of two-step processes in ^{208}Pb(α,d)^{210}Bi are also important for ^{208}Bi.

II. EXPERIMENTAL PROCEDURES

The ^{206}Pb(α,d) experiment was performed at the Princeton cyclotron laboratory using a 48.2 MeV alpha beam. An isotopically enriched ($\geq$99%) self-supporting ^{206}Pb target with a thickness of 179 μg/cm^2 was used. The reaction deuterons were detected with a position-sensitive proportional counter in the focal plane of a

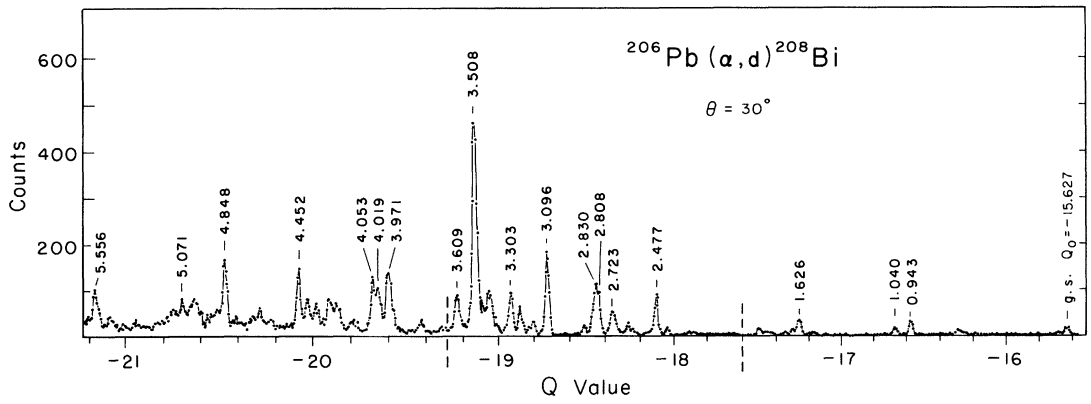

FIG. 1. Composite ^{206}Pb(α,d)^{208}Bi spectrum as observed with a QDDD spectrograph at 30° for 48.2 MeV incident α particles. The data are plotted against the transition Q value. Dominant levels are identified by their excitation energy in MeV. A normalized average of 25° and 35° spectra was substituted for small regions near $Q=-18$ and -19.8 MeV which at 30° were obscured by broad ^{12}C(α,d) and ^{16}O(α,d) impurity peaks.

TABLE I. Comparison of known properties of ^{208}Bi with results from the present work.

Previous work						Present work			
NDS[a] (keV)	(p,d)[b] (keV)	(^{3}He,d)[c] (keV)	l	G	NDS[a] J^π	(α,d)[d] (keV)	σ_{max} (μb/sr)	L[e]	J^π
0.0	0.0	0.0	5	5.5	5^+	0.0	12.5	6	
63.3	63.4	65	5	4.1	4^+	62	1.7	4	
510.6	511.4				6^+	(510)			
601.8	603.0	603	(5) or 3	0.76 0.09	4^+				
628.6 633.5	631.8[f]	631	(5) or 3	0.83 0.11	5^+ 3^+	(632)[f]	(1.9)		
650.7	652.3				7^+	657[f]	(4.8)		
886.7	888.6				5^+	888	(2.3)		
925.2	927.3				2^+				
936.6		939	3	3.4	3^+	943	(8.4)	(4)	
959.3	961.2				4^+				
1033.6	1035.6	1038	3	3.9	4^+	1040	5.7	4	
1069.5	1071.2				3^+				
1094.5	1097.4				6^+				
1384.3					$(3^+,4,5^+)$				
1435.7									
1469.8					$(4^+,5^+)$	1474	2.5		
1529.8					$(2^+,3,4^+)$				
	1533.5					1535	2.4	(3)	
1539.8					$(2^+,3,4^+)$				
1563.8		1565	3	0.18	$(3^+,4,5^+)$				
1571.1	1575.6				10^-	1578	0.9		
1606									
1629	1628.8	1630	6	5.9	6^-	1626	12.2	5	
1636.9									
1664	1664.1				8^-				
1666.2									
1673		1673	6	5.6	7^-	1669	10.2	7	
1703.5	1708.2				5^-				
1721	1720.6	1719[f]	6	2.1	6^-+7^-	1717	5.8	(6—9)	
1734									
1792	1791.5				9^-				
1802.5									
1805		1806	(3)	0.31		(1807)	~3		
1837.2					$(4^+,5,6^+)$	1840	7.7	(6)	
1844.2	1843.9				4^-				
1876	1875.7								
		1885	(3)	0.30		1885	5.0	(5)	
1920.5					$(3^+,4^+)$				
1925	1924.7				3^-				
1938.0									
2077.9									
2132		2132	(1)	0.08					
2137									
2165									
						2250	3.6	(5)	
2308.7									
2346	2345.9				7^+				
2391	2391.2				4^++5^+				
2401.6									
2413 2415	2414.9				9^- 6^+	2417	13	(6—9)	
2434	2434.2				11^-				
2464	2463.5	2462	(3)	0.17	3^+				
2475					9^-	2477	58	9	(9^-)
2508	2507.7	2506	(3)	0.11	2^+	2514	5.8		
2560						2609	11		
						2641	20		

TABLE I (*Continued*).

Previous work					Present work				
NDS[a] (keV)	(p,d)[b] (keV)	(^{3}He,d)[c] (keV)	l	G	NDS[a] J^π	(α,d)[d] (keV)	σ_{max} (μb/sr)	L[e]	J^π
2668	2667.5				8^+				
2688									
2716									
2723						2723	30	(5+7)	
2727	2727.0								
2808					(10^-)	2808	43	11	(10^-)
2830						2830	54	(7)	
2850									
2888					1^+				
2890	2891.6	2890	3	3.4	3^+	2892	6.1		
2892					1^+				
2901									
(2915)									
2945		2945	3	2.8	2^+				
3057	3057								
3070		3070	1	0.19	(1^+,2^+)				
3079	3079								
3096						3096	114	7	(8^-)
3099									
3122	3122								
3149	3149								
3162									
3173		3173	1	0.76	(1^+,2^+)	3176	11		
						3211	6.3		
3220	3220								
3248	3248					3250	31		
3260		3260	1	0.48	(1^+,2^+)				
3261									
3270									
3281	3281								
3288		3288	1	1.68	(1^+)				
						3303	48		
3310									
3326	3326								
3335	3335				(4^-,5^-)	3334[f]	7.6		
3340									
3355	3355				(4^-,5^-)				
3371	3371								
						3383	20		
3396	3396								
3410		3410	1	0.44	(1^+,2^+)				
3421	3421								
3460		3460	1	0.32	(1^+,2^+)	3454[f]	60		
3462									
3473	3473								
3508						3508	236	10	(11^+)
3530	3533	(3535)[h]			9^-				
3533									
3550	3550					3551	19		
3572									
3574	3574								
3609					(12^+)	3609	32	(12)	(12^+)
3612		3612	1	0.60	(1^+,2^+)				
3620	3620								
3640									
3671	3671								
3697	3697								
3732	3732								

TABLE I (*Continued*).

Previous work					Present work				
NDS[a] (keV)	(p,d)[b] (keV)	(^{3}He,d)[c] (keV)	l	G	NDS[a] J^π	(α,d)[d] (keV)	σ_{max} (μb/sr)	L[e]	J^π
3751	3751								
3761									
3776	3776								
						3799[f]	25		
3861						3858	(7.4)		
3896	3896								
3916						3909	(4.4)		
3971						3971	74		
4019						4019	(43)		
4025	4025								
4053						4053	(54)		
4097									
4147						4160[f]	(14)		
4194	4194								
4249						4240[f]	(38)		
						4288	(52)		
						4361	(29)		
						4403	(29)		
4452						4452	55		
4555	4555								
4568	4568								
4599	4599								
4629	4629								
						4656	24		
						(4701)[g]	(21)		
4848					(14$^-$)	4848	38	(13)	(14$^-$)
						4889	19		
						5012	29		
5071						5071	31		
						5467[f]	17		
5556						(5556)[g]	42		

[a]Reference 11; most J assignments are tentative.
[b]Reference 6.
[c]Reference 5.
[d]Excitation energies are uncertain to ±0.2% or 3 keV, whichever is larger.
[e]These (α,d) L values are only determined to within one or two units from the angular distribution. Additional information was used for the L assignment.
[f]Doublet.
[g]Seen at only three angles.
[h]Weak.

quadrupole-dipole-dipole-dipole (QDDD) spectrograph. A NaI detector monitoring the elastically scattered alpha particles was used to normalize the data. This monitor, fixed at $\theta=60°$, was also used to assess target quality during the experiment.

Due to the large dispersion of the QDDD spectrograph and the large negative (α,d) Q value of -15.627 MeV, only 2 MeV of excitation energy was detectable for a given magnetic field setting. Therefore, data for each angle were taken at three different magnetic field settings on the QDDD with an E^* overlap of several hundred keV between adjacent settings to aid in the energy calibration and peak identification. Angular distributions were taken in 5° steps from $\theta_{lab}=10°$ to 40°. A deuteron energy resolution of 25 keV FWHM was obtained. The main contributions to this resolution were target thickness and beam energy spread.

A typical (α,d) spectrum is shown in Fig. 1. This is a composite plot of the three magnetic field settings used for $\theta_{lab}=30°$. The peak fitting program AUTOFIT (Ref. 10) and hand analysis were used for the data reduction including energy calibration and background subtraction. Some ^{208}Bi peaks were obscured by $^{16}O(\alpha,d)^{18}F(5^+,3^+)$ and $^{12}C(\alpha,d)^{14}N(3.95$ MeV) impurity transitions and resulted in missing data points in the angular distributions. Cross section uncertainties are primarily due to errors in separating poorly resolved levels, background subtraction, and peak count statistics. Absolute scale errors arose primarily from uncertainties in the charge integration and target thickness, and are estimated to be about ±20%.

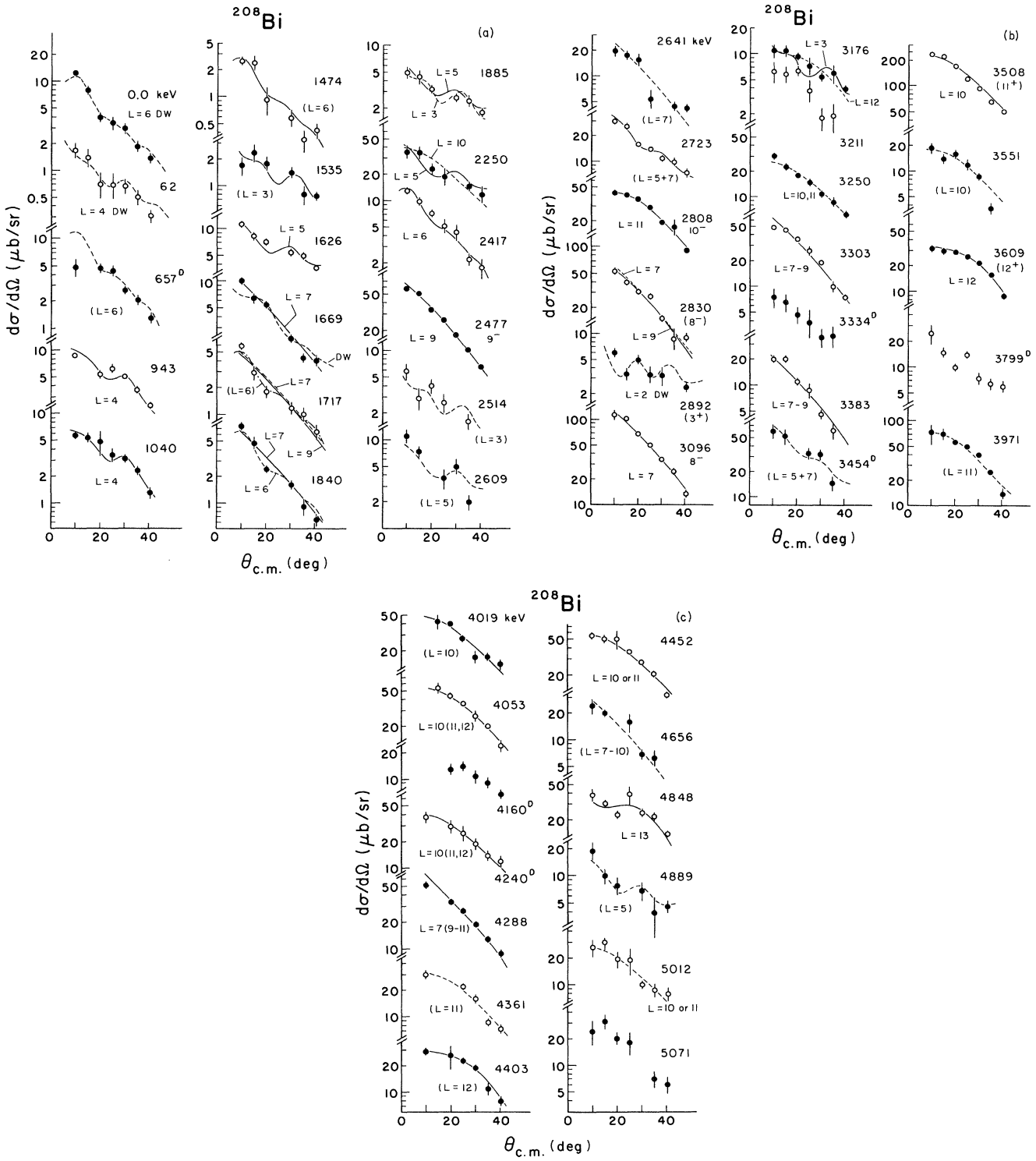

FIG. 2. ^{206}Pb(α,d)^{208}Bi angular distributions measured at 48.2 MeV. Data are compared with empirical curves deduced at similar Q values from known transitions. The L values shown gave the best (but not the only) acceptable fits. For new levels, L is generally uncertain by ± 1 unit. Error bars give uncertainties from statistics and background subtraction. Level energies are given in keV. Solid lines are empirical curves, the dashed lines indicate DWBA or more tentative fits.

III. EXPERIMENTAL RESULTS

Table I lists the ^{208}Bi energy levels obtained from this ^{206}Pb(α,d) experiment in comparison with results from previous single-particle transfer measurements.[5,6,11] The (α,d) excitation energies (E^*) for resolved states are uncertain to the larger of $\pm 0.2\%$ of E^* or 3 keV. The sixth column lists the previously assigned J^π values where known and the eighth column gives the maximum (α,d) cross section observed (typically at $\theta = 10°$). The

parentheses for some of the σ_{max} values indicate that the largest cross section may not have been seen since some low angle data points for these peaks are missing due to impurities, etc. Where it is certain which levels populated by (α,d) transitions correspond to previously reported levels, the agreement in E^* is good. For higher excitations, correspondence to (^{3}He,d) transitions is expected, but agreement with (p,d) energies may be spurious.

The (α,d) reaction favors transitions with relatively large L transfers, and angular momentum matching considerations and DWBA calculations predict that for 48 MeV alpha particles, ^{206}Pb(α,d) transfers of $L=6$—10 are dynamically favored.[7] One does not expect to strongly excite low spin states in ^{208}Bi. Angular distributions for the levels populated in ^{208}Bi are given in Figs. 2(a)—2(c); those with fewer than five data points are not shown. Angular distrubitions for $L>5$ are rather structureless, and a distinct forward angle peaking is the dominant characteristic. Generally, larger cross sections and a steeper fall-off with θ are seen for $7\leq L\leq 9$. The error bars shown indicate statistical and background subtraction errors.

The spectrum in Fig. 1 shows enhancement of several levels with $(j_1+j_2=J_{max})$ structure, especially the 3.508 ($J^\pi=11^+$) MeV level along with levels at 2.477 MeV ($J^\pi=9^-$), 2.81 MeV ($J^\pi=10^-$), 3.096 MeV ($J^\pi=8^-$), 3.609 MeV ($J^\pi=12^+$), and 4.848 MeV ($J^\pi=14^-$). These states were previously identified[7] as J_{max}, two-particle—two-hole states. As can be seen in Fig. 1 and Table I, for $E^*\geq 2.4$ MeV ($Q\leq -18$ MeV), there are additional levels which show rather large (α,d) cross sections. They are dominant over the many unresolved levels expected at these excitation energies. This would indicate that they, too (like the J_{max} levels), have a simple structure and are populated with large L transfers, although firm L values could not be assigned due to the lack of angular distribution structure. Figure 3 shows a higher resolution comparison (at 33 MeV) with a corresponding ^{208}Pb(α,d)^{210}Bi spectrum. The Q-value slice chosen includes the $(\pi h_{9/2}\nu g_{9/2})$ ground state multiplet (marked as levels 0—9) and the distinctive $(h_{9/2}i_{11/2})_{10^-}$ (No. 11) and $(f_{7/2}g_{9/2})_{8^-}$ J_{max} states (No. 12) in ^{210}Bi. At very nearly the same Q values (the drawings are shifted by 140 keV), the ^{206}Pb(α,d)^{208}Bi spectrum yields a very similar finger print. The 8^-, 9^-, and 10^- levels can be correlated on the basis of their strengths and angular distributions. It is likely that the other strong peaks in this region are also related to the ^{210}Bi structure, at least in the sense that they are dominantly two-particle (two-hole) states primarily involving the corresponding ^{210}Bi two-particle (p-n) configurations. The low-lying levels in ^{208}Bi are weaker by about an order of magnitude. Figure 4 shows a spectrum of the first 2 MeV of excitation in ^{208}Bi with an enlarged vertical scale. The peaks have been labeled with their known multiplet structure and excitation energy. The curves through the data points are fits provided by the code AUTOFIT. The J^π assignments for the low-lying levels are known from the literature.

Many previously unknown levels have been observed above $E^*=2.4$ MeV. They are identified in Table I by their measured excitation energies. Where possible, dominant L transfers have been suggested. However, the

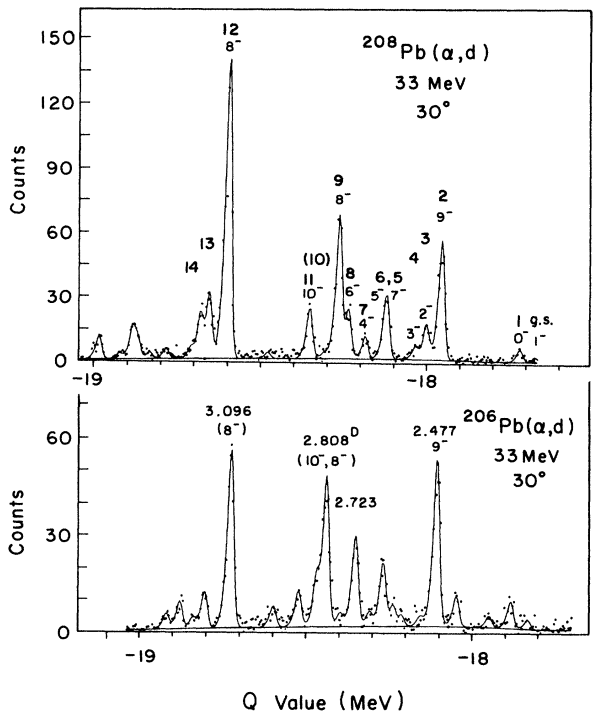

FIG. 3. Comparison of states in the 2p-2h excitation region in ^{208}Bi with a ^{208}Pb(α,d)^{210}Bi spectrum showing the low-lying n-p two-particle states. Both spectra were taken at 33 MeV. The spins of the energy correlated (J_{max}) states in the two spectra are identical. Other strong states (higher J) also seem correlated.

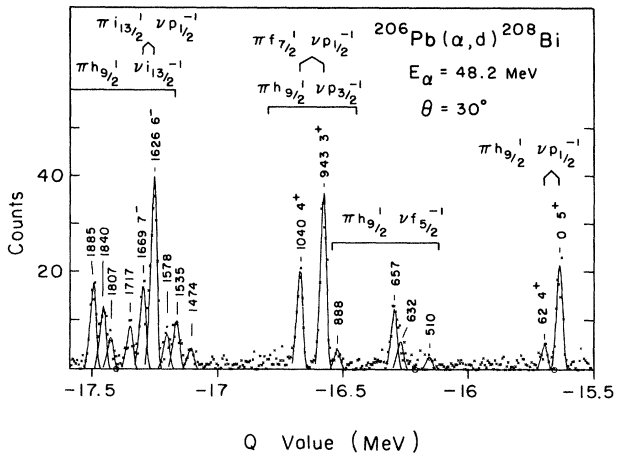

FIG. 4. Expanded spectrum for the first two MeV excitation for the ^{206}Pb(α,d)^{208}Bi reaction at $\theta=30°$. The six levels studied with the DWBA and CCBA calculations are labeled with their respective J^π and configuration assignments. Additional configurations have been indicated in the energy regions where they are expected. Three doublets dominate the spectrum in this region as expected from the predicted strength of the $|\nu p_{1/2}^{-2}\rangle$ term in the ^{206}Pb ground state wave function.

empirical fits shown in Fig. 2 are rarely unique. In particular, angular distributions for $6 \leq L \leq 9$ are hard to distinguish from each other, as are those for $10 \leq L \leq 12$. When statistics are below average, several curves give comparable fits.

Some DWBA curves are shown in Fig. 2 (identified by DW) for a number of known levels. Agreement to 20% or better is typical for $L \leq 6$. For $L \geq 7$, DWBA curves do not rise as fast with decreasing θ as do the data, and such DWBA curves do not permit a reliable identification of unknown L transfers.[7] We have used empirical curves to make L suggestions in Fig. 2 and, where available, we have taken into account spectroscopic information from the ^{207}Pb(^{3}He,d)^{208}Bi study.[5] We have also used the DWBA predicton that low spin ($J \leq 3$) final states here are not excited with cross sections above 10 μb/sr.

IV. DWBA ANALYSIS

A. DWBA microscopic one-step calculations

The shell model describes the low-lying ($E^* < 2.5$ MeV) levels of ^{208}Bi as one-proton-particle—one-neutron-hole orbits outside the doubly magic ^{208}Pb($J^\pi = 0^+$) core. The unperturbed centroids of the possible multiplets from this coupling are the sum of a single-proton particle level in ^{209}Bi and the single-neutron hole energy of the ^{207}Pb nucleus. Residual interactions are responsible for splitting the multiplet into its various perturbed levels and for some mixing of multiplets.

The (α,d) cross sections for the levels in ^{208}Bi also depend on the ground state configuration for the ^{206}Pb wave function which theory[12] and experiment[13] indicate to be strongly configuration mixed. For example, Kuo and Herling calculated (approximation II in Ref. 12)

$$\psi_{^{206}\mathrm{Pb}}(\text{g.s.}, J^\pi = 0^+) = -0.657\,|\,2p_{1/2}^{-2}\rangle - 0.474\,|\,1f_{5/2}^{-2}\rangle - 0.383\,|\,2p_{3/2}^{-2}\rangle + 0.332\,|\,0i_{13/2}^{-2}\rangle + \text{smaller terms}\ .$$

This wave function is in reasonable agreement with stripping experiments, and it was used in the DWBA calculations reported here.

The six levels expected to be seen prominently in the low-lying ^{208}Bi excitation region result from the coupling of an (excited) proton orbit to a neutron hole. In ^{206}Pb(α,d), the neutron is stripped into the $2p_{1/2}$ orbit which leaves one $2p_{1/2}$ neutron hole, and the proton is stripped into one of the three lowest single-particle orbitals available ($0h_{9/2}$, $1f_{7/2}$, or $0i_{13/2}$). The six resulting levels are the strongest levels in the first 2 MeV of excitation and are indicated in Fig. 4. The degree to which other ^{208}Bi levels are populated in this energy region depends on the configuration mixing in the ^{206}Pb ground state. As can be seen in Fig. 4, other levels are quite visible, which is consistent with the expectations from the ^{206}Pb wave function used in our calculations.

Table II lists the wave functions used in the direct one-step (α,d) DWBA calculations. The symbols π and ν refer to the proton and neutron, respectively, and the superscripts (-2) and (-1) refer to two-hole and one-hole states, respectively. As Table II shows, Kuo's wave functions[1] predict rather pure $|\,\pi j, \nu p_{1/2}^{-1}\rangle$ strength for all six ^{208}Bi levels in question. (Stripping experiments confirm the high purity of the ground state doublet, although the higher doublets are not as pure as predicted.)

Zero-range DWBA calculations were performed with the coupled channels code CHUCK3 (Ref. 14) in two stages in the manner explained in detail in Ref. 9. First, using Kuo's ^{206}Pb ground state and ^{208}Bi final state wave functions, fully detailed microscopic one-step ^{206}Pb(α,d)^{208}Bi transfer amplitudes were calculated in zero range and

TABLE II. Wave functions used in microscopic DWBA analysis of ^{208}Bi (very small terms are omitted) from Refs. 1 and 12.

E^*_{keV}	J^π	
0 Ground state	0^+	$\psi(^{206}\mathrm{Pb}) = -0.657(\nu p_{1/2}^{-2}) - 0.474(\nu f_{5/2}^{-2}) - 0.383(\nu p_{3/2}^{-2}) + 0.332(\nu i_{13/2}^{-2}) + \text{smaller terms}$
0 Ground state	5^+	$\psi(^{208}\mathrm{Bi}) = -0.990(\pi h_{9/2}, \nu p_{1/2}^{-1}) + 0.128(\pi h_{9/2}, \nu f_{5/2}^{-1}) + 0.041(\pi h_{9/2} \nu p_{3/2}^{-1}) + 0.022(\pi h_{9/2} \nu f_{7/2}^{-1})$
62	4^+	$\psi(^{208}\mathrm{Bi}) = -0.956(\pi h_{9/2}, \nu p_{1/2}^{-1}) + 0.221(\pi h_{9/2}, \nu f_{5/2}^{-1}) - 0.184(\pi h_{9/2}, \nu p_{3/2}^{-1})$
943	3^+	$\psi(^{208}\mathrm{Bi}) = +0.968(\pi f_{7/2}, \nu p_{1/2}^{-1}) + 0.145(\pi h_{9/2}, \nu p_{3/2}^{-1}) - 0.136(\pi f_{7/2}, \nu f_{5/2}^{-1}) + 0.119(\pi f_{7/2}, \nu p_{3/2}^{-1})$
1040	4^+	$\psi(^{208}\mathrm{Bi}) = -0.948(\pi f_{7/2}, \nu p_{1/2}^{-1}) + 0.230(\pi f_{7/2}, \nu f_{5/2}^{-1}) + 0.206(\pi f_{7/2}, \nu p_{3/2}^{-1})$
1626	6^-	$\psi(^{208}\mathrm{Bi}) = +0.979(\pi i_{13/2}, \nu p_{1/2}^{-1}) - 0.180(\pi i_{13/2} \nu f_{5/2}^{-1}) - 0.047(\pi f_{7/2}, \nu i_{13/2}^{-1})$
1669	7^-	$\psi(^{208}\mathrm{Bi}) = +0.953(\pi i_{13/2}, \nu p_{1/2}^{-1}) - 0.232(\pi i_{13/2}, \nu f_{5/2}^{-1}) - 0.146(\pi i_{13/2}, \nu p_{3/2}^{-1}) + 0.115(\pi h_{9/2}, \nu i_{13/2}^{-1})$

TABLE III. The optical model parameters used in the ^{206}Pb(α,d) study. The d, t, and ^{3}He parameters were obtained from global, energy dependent prescriptions as listed in the reference column. Here, E is the incident particle lab energy in MeV and $\beta=-(E/100)^2$.

Projectile	V_0 (MeV)	r_0 (fm)	a_0 (fm)	r_c (fm)	W_v (MeV)	W_D (MeV)	r_I (fm)	a_I (fm)	V_{so} (MeV)	r_{so} (fm)	a_{so} (fm)	Reference
α	169.0	1.26	0.715	1.40	37.57	0	1.26	0.82	0			9
d	$100.87-0.26E$	1.17	$0.709+0.0017E$	1.30	$(12.2+0.026E)\times(1-e^{\beta})$	$(12.2+0.026E)e^{\beta}$	1.325	0.93	$7.33-0.029E$	1.07	0.66	15(Potential L)
^{3}He	$162.1-0.17E$	1.20	0.72	1.3	$48.22-0.33E$	0	1.40	0.88	0			16
t	$163.7-0.17E$	1.20	0.72	1.3	$23.57-0.33E$	0	1.40	0.84	0			16
bound p	a	1.20	0.75	1.3					$\lambda=18$			
bound n	a	1.20	0.75	1.3					$\lambda=18$			
bound n+p	a	1.25	0.75	1.3					$\lambda=18$			

[a]Well depth adjusted by code to fit separation energy.

saved in disk files. The resulting predictions were used for a first comparison with the data.

Table III lists the optical model parameters used for the DWBA calculations. The optical potentials used for d, t, and ^{3}He come from global prescriptions[15,16] that fit a wide range of data and were also used for the ^{210}Bi results. The deuteron potentials were obtained from prescription L of Ref. 15. The α particle potentials used here are the set α_{II} of Ref. 9, and are extrapolated from a fit to 58 MeV Pb(α,α) data. For the ^{3}He potentials of Ref. 16, the isospin term in the imaginary volume potential was modified from $44(N-Z)/A$ to $32(N-Z)/A$ to fit heavier mass data[9] since the global ^{3}He potentials were obtained from fits to nuclei with $A<120$.

Table IV shows two results of the direct one-step mixed configuration (α,d) calculations for the six well-known levels. Experimental and predicted results are compared through their integrated cross sections σ_{int}. The unfavored L transfers, where present, have been included but make a very small contribution to the overall results. The $\sigma_{\text{int}}^{\text{theory}}$ values were computed using zero-range normalization constants of $N=4800$ and 3600. $N=4800$ was the value for N determined in the ^{210}Bi paper. As can be seen in Table IV, with this normalization DWBA overpredicts five of the six levels. The overprediction is particularly serious for the $J_{\max}$ members of the doublets. The zero-range normalization constant N is not well known and is dependent on the intrinsic alpha and deuteron wave functions, and on the optical parameters used. Hence, N for (α,d) reactions has usually been determined empirically, and $N=3600$ is a better choice for ^{208}Bi. The implication that N may not stay constant for neighboring isotopes or from one known state to another in ^{208}Bi and that it gives relative predictions significantly different from the experimental results should cause some concern. It is unlikely that this effect can be explained by our use of the extrapolated α scattering potentials since the same potentials were used successfully for the ^{208}Pb(α,d)^{210}Bi calculation.

Figure 5 illustrates the DWBA (α,d) predictions for integrated cross sections. The experimental data points are shown with their error bars. The dash-dot horizontal lines indicate the one-step results for $N=3600$. It is seen that the $J_{\max}$ levels of the three doublets are all significantly overpredicted by DWBA whereas the other three levels are underpredicted. In order to cross check the optical model parameters used here, calculations were performed for several strong and previously identified $J_{\max}$ two-particle–two-hole states in ^{208}Bi, namely the $J^{\pi}=9^-$ and 10^- levels at 2477 and 2808 keV, respectively. The results are consistent with the corresponding $J_{\max}$ cases for the ^{210}Bi data. Hence it does not appear that the optical parameters used are less appropriate for ^{206}Pb than they were for ^{208}Pb. The overprediction of the $J_{\max}$ states is, however, reminiscent of similar systematics in ^{210}Bi, and prompted us to supplement the one-step calculations by further calculations which included sequential stripping channels.

B. Coupled-reaction channel two-step calculations

The most important two-step channels for ^{206}Pb(α,d)^{208}Bi are the sequential stripping channels

TABLE IV. ^{206}Pb(α,d)^{208}Bi microscopic zero-range mixed configuration one-step DWBA results (integrated for $7.5° \leq \theta \leq 42.5°$) and a more complete calculation including two-step channels, compared with experiment. CCBA stands for coupled-channel Born approximation.

E^* (keV)	J^π	L	Dominant configuration (π,ν^{-1})	$\sigma_{\text{int}}^{\text{exp}}$ (μb)	σ Theory One step $N=3600$	One step $N=4800$	CCBA $N=3600$
0	5^+	6	$(0h_{9/2},2p_{1/2}^{-1})$	5.80±0.72	9.4	16.8	14.2
		4			0.02	0.05	
62	4^+	4	$(0h_{9/2},2p_{1/2}^{-1})$	1.10±0.29	0.89	1.57	1.26
943	3^+	2	$(1f_{7/2},2p_{1/2}^{-1})$	7.71±0.76	3.5	6.24	5.1
		4			0.13	0.24	
1040	4^+	4	$(1f_{7/2},2p_{1/2}^{-1})$	5.07±0.88	6.7	11.9	8.4
1626	6^-	5	$(0i_{13/2},2p_{1/2}^{-1})$	9.30±0.83	7.5	13.3	12.7
		7			0.13	0.22	
1669	7^-	7	$(0i_{13/2},2p_{1/2}^{-1})$	5.22±0.58	12.3	21.9	18.2

(a) ^{206}Pb(α,t)^{207}Bi(t,d)^{208} Bi

and

(b) ^{206}Pb(α,^{3}He)^{207}Pb(^{3}He,d)^{208} Bi .

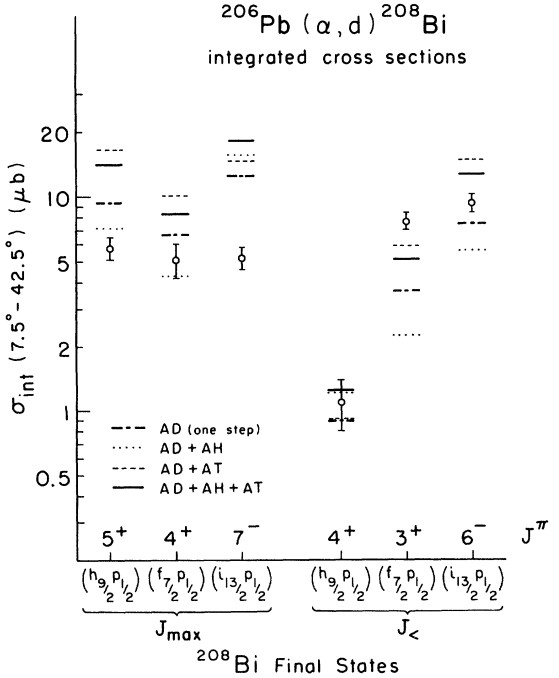

FIG. 5. Graph of the DWBA one-step and CCBA two-step results. The integrated cross sections (σ_{int}, from 7.5° to 42.5°) are compared to the corresponding experimental values. The dashed-dot lines show the one-step (α,d) results. The solid bars represent the coherent sum of the one-step plus the two-step contributions. The dotted lines give results where the (α,^{3}He,^{3}He,d) transition amplitude only has been added to the one-step amplitude. The dashed lines refer to the corresponding partial sum of (α,t;t,d) plus one-step amplitude. A zero-range (α,d) normalization constant of $N=3600$ was used.

For each transition to a given final state of configuration $|jp_{1/2}^{-1}\rangle$ two intermediate states of the nucleus seem most important: the ground state of ^{207}Pb for channel (b) and the simple p-h ($\pi j\, \nu p_{1/2}^{-2}$) state of ^{207}Bi for channel (a). Only these states were included in the two-step calculations, in analogy to the earlier work for ^{208}Pb(α,d). However, it must be cautioned that this simplification is less easily justified for ^{206}Pb(α,d) than was the exclusive use of j_1,j_2 intermediate states for ^{208}Pb(α,d). Although the ^{208}Bi wave functions are predicted to be as pure as those for ^{210}Bi, ^{206}Pb is not as simple a target as ^{208}Pb and the assumption of $|^{206}\text{Pb}\rangle \approx 0.66\,|p_{1/2}^{-2}\rangle$ for the two-step calculations is a very rough approximation.

The second order two-step contributions can be estimated from the wave functions of Table II. For instance, for the population of the 1040(4^+) state the spectroscopic amplitude for the dominant ($f_{7/2}p_{1/2}$) two-step contribution (which we included) is proportional to $c_1=1\times0.657\times0.948=0.623$. The neglected ($f_{7/2}f_{5/2}$) two-step amplitude is proportional to $c_2=\sqrt{(2/6)}\times0.474\times0.230=0.063$. Hence it is about an order of magnitude smaller than the dominant one. On the other hand, the ($f_{7/2}p_{3/2}$) amplitude is proportional to $c_3=\sqrt{(2/4)}\times0.383\times0.206=0.056$. It is comparable to c_2 and must be kept if c_2 is kept. Two further two-step terms may also contribute in this higher order. Hence a more complete calculation than the one reported here would be quite time consuming and perhaps not even of any greater quantitative significance given the tentative nature of the higher terms in the ^{208}Bi wave functions. For these reasons, only the dominant two-step term was kept. We caution, however, that in a case of extreme interference the neglected terms may well change the total predicted cross sections by about 50%.

The computed two-step cross section was found about a factor of 2—4 [depending on $N(\alpha,\text{d})$] smaller than the corresponding one-step ^{206}Pb(α,d) term, which again is comparable to the ^{208}Pb case.[9] We refer to Ref. 9 for a detailed discussion of the coupled reaction channel calcu-

lations, including questions concerning spectroscopic amplitudes, optical model potential considerations, and the externally entered phase factors for the code CHUCK3. The calculations reported here followed the same pattern: The one-step term was the largest one and computed in full microscopic detail. The two-step amplitudes included only the two largest channels. They were computed separately, stored in disk files, and later combined with the stored one-step amplitudes in a coherent sum of all channels using the program SUMAMP (Ref. 17). Two-step channels with reduced spectroscopic amplitudes and higher order reaction channels were neglected.

Table V gives the spectroscopic amplitudes and reordering phases not contained in CHUCK3, which had to be entered by hand in order to ensure that the various CHUCK channels generated phase equivalent final states. In addition, the published shell-model wave functions used here[1,12] follow a different sign convention than CHUCK3 and were adjusted to make them compatible. The values used for the stripping spectroscopic amplitudes were as determined in the ^{210}Bi study.

Figure 5 also contains the calculated two-step results. The solid lines show the integrated cross sections obtained from the coherent sum of the one-step (α,d) and two-step amplitudes, the dashed and dotted lines give partial cross sections. The modification of $\sigma_{\rm int}^{\rm theory}$ by the contribution of the two-step calculations is appreciable for the levels in question. However, for all six levels the effect of including two-step channels is to enhance the one-step results by factors from 1.2 to 1.7. This is unlike the ^{210}Bi results where constructive and destructive interference alternated for the ten members of the $(\pi h_{9/2}\nu g_{9/2})$ multiplet. The predicted (α,t;t,d) channel cross sections here are by about a factor of 2 smaller than the one-step (α,d) values. As in ^{208}Pb(α,d), the ^{206}Pb(α,^{3}He;^{3}He,d) channel cross sections are about an order of magnitude smaller than the (α,t;t,d) results. Small ($\sim\pm$20%) changes were made in the (α,d) one-step normalization to see if the coherent summations were very sensitive to these changes. They were not. Finally, as was discussed in the ^{210}Bi paper, the (α,^{3}He;^{3}He,d) amplitudes were enhanced (here by a factor of 2) to test their effect on the overall sum. For this case, some moderately destructive interference effects ($\lesssim$20%) were seen for four of the six levels.

Figure 6 shows the DWBA calculations for the angular distributions for the six low-lying particle-hole states in ^{208}Bi under discussion. The solid lines represent the microscopic one-step predictions. The dashed curves are obtained from a coherent sum of the one-step and two-step amplitudes with the phases and spectroscopic amplitudes as listed in Table V. Both sets fit the experimental angular distributions similarly well after they were renormalized individually to the data. The addition of the two-step channels here and elsewhere changes the angular distribution slightly.

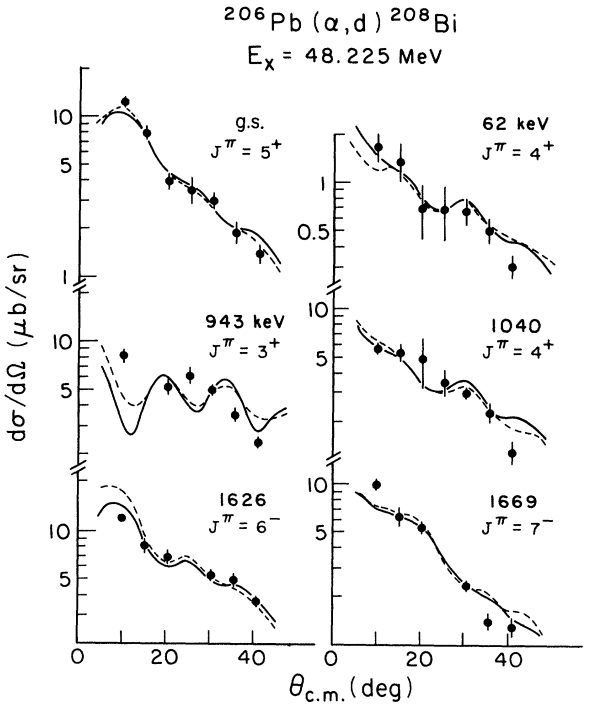

FIG. 6. Angular distributions for the six low-lying levels in ^{208}Bi for which detailed DWBA and CCBA calculations were performed. The solid curves are the zero-range one-step DWBA mixed configuration results. The dashed curves are the predictions from a coherent sum of the one-step plus the two-step contributions ^{206}Pb(α,t;t,d) and ^{206}Pb(α,^{3}He;^{3}He,d). Both one-step and two-step calculations were made using the code CHUCK3. (All curves were individually normalized to the data.)

TABLE V. The spectroscopic amplitudes and phases used for the direct (α,d) and two-step path calculations with the program CHUCK3. These values were discussed in Ref. 9. Here, j_1 and j_2 are the total angular momenta of the transferred proton and neutron and J is the total angular momentum of the final state in ^{208}Bi. ($CS^{1/2}$ is the spectroscopic amplitude for the projectiles and D_0 is the CHUCK zero-range normalization.)

Channel	Phase $\times(CS^{1/2}D_0)_1\times(S^{1/2}D_0)_2$			
(α,d)		3600 or 4800		$j_1\neq j_2$
(α,t;t,d)	$(-1)^{j_1+j_2-J}$	(−735)	(−226)	
(α,^{3}He;^{3}He,d)	−1	(+707)	(−237)	

V. DISCUSSION

A. Comparison of experiment and calculations

The simple $|0,\nu p_{1/2}^{-2}\rangle_{0^+}$ structure assumed for ^{206}Pb in our two-step calulations is not found in nature and very detailed agreement with experiment is not expected. Nevertheless, the (α,d) measurements and calculations for the states of Fig. 5 should and do exhibit some characteristic behavior that merits further discussion. The spectrum of Fig. 4 shows that the six levels in ^{208}Bi, which are interpeted in first order as pure $(h_{9/2}p_{1/2}^{-1})$, $(f_{7/2}p_{1/2}^{-1})$, and $(i_{13/2}p_{1/2}^{-1})$ multiplets,[5] constitute the more strongly excited states below 1.8 MeV excitation. Their angular distributions are reproduced well (Fig. 6), and their integrated cross sections are reproduced to within a factor of 2 by microscopic one-step DWBA calculations (if $N=3600$ and Kuo-Herling[12] and Kuo[1] wave functions are used) (see Fig. 5). Reminiscent of ^{208}Pb(α,d)^{210}Bi,

there are systematic differences in detail: DWBA overpredicts all three J_{max} states and underpredicts their $J=J_{max}-1$ partners. As in ^{208}Pb(α,d), the inclusion of the dominant two-step channels changes the DWBA predictions by about a factor of 2 (see Fig. 5).

However, the two studies differ in other respects:

(a) The theoretical wave functions may be less reliable here. The purity of the $(6^-,7^-)$ multiplet is lower and varies more than suggested by the calculations of Ref. 1 listed in Table II; e.g., the (^{3}He,d) measurements of Ref. 5 (summarized in Table I), suggest a value of 0.864 for the $(i_{13/2}p_{1/2}^{-1})_{7^-}$ amplitude, rather than the value 0.953 predicted (Table II) and used in the calculations.

(b) The ^{206}Pb(α,d)^{208}Bi ground state Q value is $Q=-15.627$ MeV, i.e., 2.042 MeV less negative than the ^{208}Pb(α,d) value of $Q=-17.669$ MeV. While this difference does not necessarily suggest problems for an experiment at 48 MeV, the need for a significant reduction of the one-step (α,d) zero-range CHUCK normalization (from 4800 to 3600) is unexpected and points towards a Q-value sensitivity. We note that no DWBA renormalization seems needed for the 10^- state at 2.808 MeV which is presumed to have the rather pure configuration $|^{206}\text{Pb},\pi h_{9/2}\nu i_{11/2}\rangle$; but this state has the same Q value as the corresponding state in ^{210}Bi.[7]

(c) In contradistinction to the results of Ref. 9 for ^{208}Pb(α,d)^{210}Bi, the inclusion of the dominant two-step amplitudes for ^{206}Pb(α,d) transfers to the low-lying doublets results only in enhancements for the predicted cross sections. As shown in Fig. 5, the enhancement factors differ considerably from state to state, but none was smaller than 1.25. We note parenthetically that even an arbitrary change of the relative phases of the three different transition amplitudes could produce only one significant decrease in the six predictions.

It seems necessary to conclude that the DWBA calculations discussed above predict the ^{206}Pb(α,d)^{208}Bi data only in a rough and qualitative way. The inclusion of the dominant two-step channels in second order DWBA produces some noticeable changes for individual transfers; however, overall agreement is not improved. Significantly stronger configuration mixing in the ^{206}Pb ground state than that given in Table II could result in DWBA predictions more like the data, but there is no independent evidence to support a change in the ^{206}Pb wave function.

B. Channel phases and nuclear distortions

In a discussion of the two-step calculations for (α,d) reactions, Pinkston and Satchler[18] implied that the channel phases used in Ref. 9 may be in error. As given in Table V, these phases supplement the computer program CHUCK3 so that it will generate identical final states while calculating the different one- and two-step transition amplitudes. CHUCK3 is a reaction code and essentially ignores the nuclear structure aspects of the problem. All spectroscopic amplitudes and the reordering phases have to be entered by the user.[14] In two-step (α,d) transfers CHUCK3 generates final states that differ from each other[9] by a reordering phase $-(-1)^{j_1+j_2-J}$. There are other phase factors that occur throughout the computations, but they tend to cancel for inert core target nuclei so that apart from the phases of configuration-mixed wave functions, only the reaction code phases of Table V survive for ^{206}Pb(α,d). This statement assumes that the wave functions entered are written in the reaction convention, which differs from some (e.g., Kuo's) shell model conventions by $(-1)^{n_1+n_2}$ and $i^{l_1+l_2}$ factors. The phases of Table V have been checked in bench-mark calculations [e.g., for $(j^2)_{J=\text{even}}$ transfers that must have very small or vanishing cross sections even though the individual two-step channels can have large cross sections]. They have recently been rederived from a study of the program source file. No errors were found.[19] Testing additional cases, it was found that the phases of Table V lead to very successful calculations for other "pure" multiplets, e.g., $(\pi g_{9/2}\nu d_{5/2})$ in ^{98}Mo(d,α)^{96}Nb and $(\pi f_{7/2}\nu p_{3/2})$ in ^{48}Ca(α,d)^{50}Sc, whereas one-step DWBA fails. Such agreement is gratifying and suggestive. It does not, of course, prove or disprove a theoretical argument, and further efforts at understanding the apparently contradictory theoretical results of Refs. 9 and 18 are called for. Unfortunately, the calculational approach of CHUCK3 (plus Ref. 9) has to be very different from the formal one of Ref. 18, so that a direct comparison is difficult. We mention here that some nuclear labels considered in Refs. 9 and 20 are not displayed in the formalism of Ref. 18. They may have been ignored where ordering had to be considered. The suppression of a (J dependent) reordering phase could lead to a J-independent formalism, and hence to the contradiction. This question will be pursued further elsewhere.[20]

There may be a second source for conflicting conclusions. Reference 18 observes that in the closure approximation for the intermediate nuclear states, the same nuclear structure overlaps enter into both the one-step and the two-step overlaps. The light-ion overlap function $D(r)$ in the one-step process is replaced by a Green's function $\bar{\bar{G}}=\bar{G}^{(t)}+\bar{G}^{(h)}$ consisting of the triton and helion propagators. Usually, $D(r)$ is assumed to be real, where $\bar{\bar{G}}$ is complex. It was argued in Ref. 18 that the differences in the operators are secondary and do not cause, in first order, J dependent effects for the combined amplitudes; hence any computed J effects should come from spurious phases. Reference 18 and subsequent communications from its authors seem to imply that the $T(\alpha,\text{d})\equiv(\text{AD})$, $T(\alpha,\text{t};\text{t},\text{d})\equiv(\text{AT})$, and $T(\alpha,\text{h};\text{h},\text{d})\equiv(\text{AH})$ transition amplitudes behave like essentially parallel or antiparallel vectors in hyperspace. While these assumptions may be realizable in some very special cases (no distortion, no $l\cdot s$ terms, identical Q values, etc.), they are greatly at variance with the numerical results for Pb(α,d) which are shown in Figs. 5, 7, and 8.

Figures 7(a) and (b) show partial and complete (zero-range) second-order DWBA differential cross sections for transitions to the two states of the $(h_{9/2}p_{1/2}^{-1})_{5^+,4^+}$ multiplet. The numerical result is that the AH two-step cross section is very much smaller than the other channels, and its addition to the AT two-step channel leads to a slight enhancement of the two-step cross section. When combined with the one-step amplitude, the two-step amplitudes lead to 50% and 35% enhancements in the 5^+ and

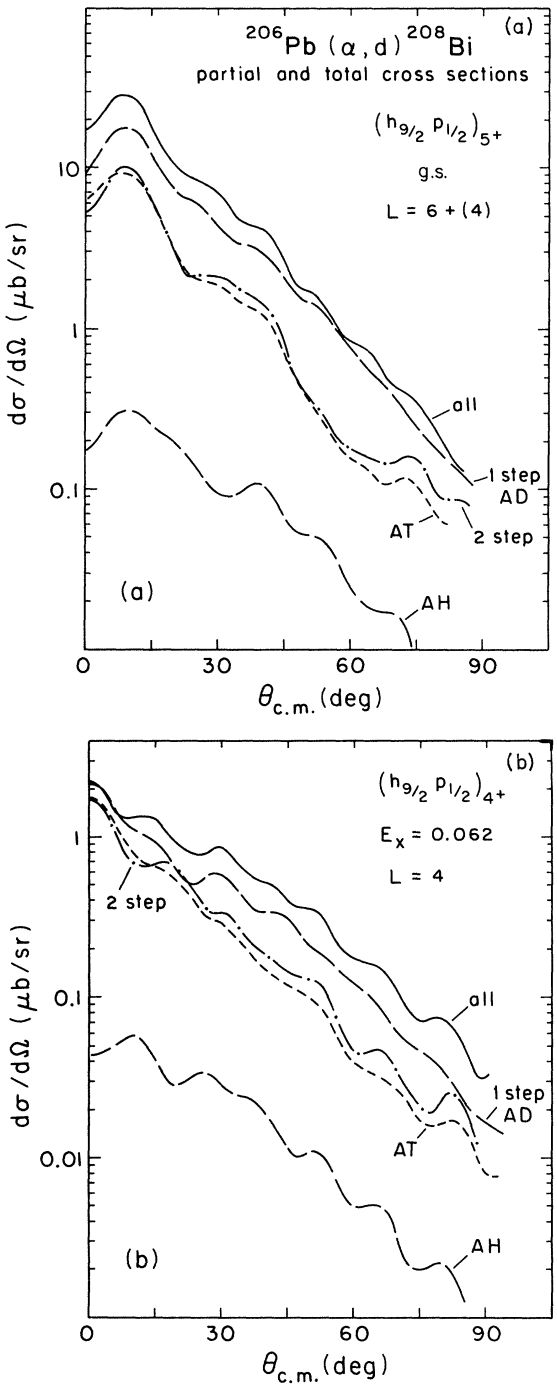

FIG. 7. Partial and total cross sections computed for the (α,d) transition to the $(h_{9/2}p^{-1}_{1/2})$ doublet. It is seen that the one-step (AD) and the two-step (α,t;t,d) branch (AT) yield the largest partial cross sections. However, the effect of the small AH branch is not negligible in the total summation.

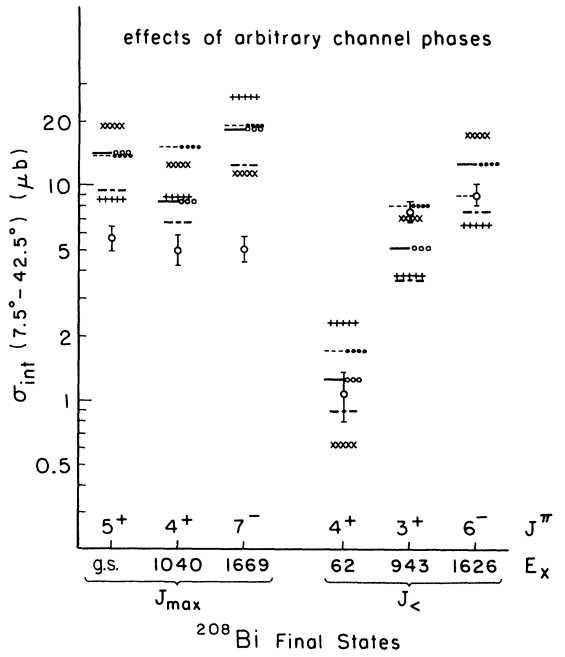

FIG. 8. Survey of the variation of cross section results (integrated from 7.5 to 42.5°) for ^{206}Pb(α,d), resulting from various arbitrary phase changes. (a) Microscopic one-step DWBA results only (dash-dotted lines). (b) Complete cross sections with phases as in Table V and Fig. 5 (solid lines). (c) Complete cross sections with J dependent phase on AH channel (dots). (d) As in (b), but direct AD channel phases reversed (dashed lines). (e) As in (c), but direct AD channel phases reversed (open circles). (f) As in (b), but with extra minus sign in AT channel (+++ symbols). (g) As in (f), but direct AD channel phases reversed (××× symbols). These assumptions include all possible permutations for each state. A significant reduction of the one-step cross section is seen only for one (4^+) state.

4^+ cross sections, respectively. Figure 7, therefore, shows primarily that the AH and AT amplitudes are of very different magnitude. The major effect of AH, if any, is hidden. In Fig. 5 the integrated (AD+AH) and (AD+AT) partial cross sections were shown by dotted and dashed lines, respectively. Here, surprisingly, we see that in these partial sums, the tiny AH amplitude modifies the AD cross section as much as the very large AT amplitude; it decreases four of the AD cross sections and enhances the two others by practically as much as expected in an addition of antiparallel and parallel vectors. We note that Table V has *no* $(-1)^J$ phase factor for AH. The (AT+AD) effect is similar in magnitude, but here it is always of the same sign for all six states, even though AT *does* have a (Table V) $(-1)^J$ phase associated with it. If the AT phase is arbitrarily reversed, (AD−AT) often yields cross sections essentially comparable to the (AD+AT) cross sections. Examples of the effect of arbitrary phase changes of the partial amplitudes are shown in Fig. 8. We conclude for Pb(α,d) that AT acts like a vector which is nearly orthogonal to AD. Hence, one may argue with some justification that AT and AH are *not* generally similar or comparable. In Pb(α,d) they differ greatly in magnitude and are nearly orthogonal. While the effect of AH would be very sensitive to an external phase factor (if there were any), the effect of AT is not dominated by its external phase.

Thus the results of arbitrary summations in Fig. 8 together with the derived ones in Fig. 5 illustrate that some of the simplifying assumptions made in the conclusions of

Ref. 18 are not permissible for (α,d) reactions in the lead region if one uses realistic nuclear distortions and Green's functions.

For the $^{206}Pb(\alpha,d)^{208}Bi$ reaction, the experimentally observed quenching of J_{max} cross sections is not reproduced by our calculations, nor could it be "manufactured" by arbitrary phase factors. More subtle effects of reaction theory, such as finite range or nonorthogonality, may have become important. We may also have used inadequate wave functions, and if so we have used too few two-step channels. One suggested refinement,[21] the inclusion of the D state in the one-step amplitude, has not been made, primarily for lack of a realistic (α,d) finite-range form factor. If this effect is as large as estimated in Ref. 21 it would help suppress the overprediction of the 4^+ and 7^- cross sections. It would, however, make worse the already poor agreement for the overpredicted 5^+ and 6^- states. Existing evidence suggests that the experimental J-dependent "sawtooth" effect seen here and in several other "pure" multiplets is not correctly explained by the D-state effect.[22] The latter always suppresses natural parity states. In the known transitions to pure multiplets, it is the state of maximum J and every alternate J, $J=(J_{max}-2n)$, that are suppressed, but the parity of these suppressed states differs from multiplet to multiplet.

VI. SUMMARY

A number of new levels in ^{208}Bi were found in the $^{206}Pb(\alpha,d)$ reaction study. Many of these levels are high spin levels since angular momentum transfers of $6 \leq L \leq 10$ are dynamically favored at this alpha energy. Most of these levels are difficult to populate in single nucleon transfer reactions by which most prior studies of ^{208}Bi have been made. The angular distributions for all levels seen were forward peaked and rather structureless. As a consequence, it was difficult to assign definite J^π and L transfer values except for those J_{max} levels previously reported and listed in Ref. 7.

Zero-range DWBA calculations for six low-lying levels in ^{208}Bi were performed in the direct one-step (α,d) mode using mixed configuration wave functions for the ^{206}Pb ground state and the ^{208}Bi final states. It was found that the J_{max} states for these three doublets were all significantly overpredicted by DWBA. Contributions of two-step sequential stripping channels to the one-step results were investigated with CHUCK3 and were found to give varying amounts of enhancement for all six levels. Unlike a similar analysis for the ^{210}Bi results, the inclusion of two-step amplitudes did not improve the agreement with the one-particle—one-hole data over that obtained using the one-step (α,d) predictions alone. There may be several reasons for the poor agreement. The best understood one is the presence of considerable configuration mixing in the four more highly excited states of the six analyzed in detail. Uncertainty in the externally entered channel phases was ruled out as a possible explanation.

ACKNOWLEDGMENTS

We gratefully acknowledge the help of Dr. W. Oelert and Dr. R. M. Del Vecchio in the initial acquisition of the data. Doctor J. R. Comfort has given much help in our dealings with CHUCK3. This work was supported by the National Science Foundation.

*Present address: Westinghouse-Bettis, P.O. Box 79, West Mifflin, PA 15122.

[1]T. T. S. Kuo, Nucl. Phys. A122, 325 (1968).
[2]Y. E. Kim and J. O Rasmussen, Nucl. Phys. 61, 173 (1965); 47, 184 (1963).
[3]C. W. Ma and W. T. True, Phys. Rev. C 8, 2313 (1973).
[4]J. R. Erskine, Phys. Rev. 110, B135 (1964).
[5]W. P. Alford, J. P. Schiffer, and J. J. Schwartz, Phys. Rev. Lett. 21, 156 (1968); Phys. Rev. C 3, 860 (1971).
[6]G. M. Crawley, E. Kashy, W. Lanford, and H. G. Blosser, Phys. Rev. C 8, 2477 (1973).
[7]W. W. Daehnick, M. J. Spisak, R. M. DelVecchio, and W. Oelert, Phys. Rev. C 15, 594 (1977).
[8]W. W. Daehnick, M. J. Spisak, and J. R. Comfort, Phys. Rev. Lett. 41, 6392 (1978).
[9]W. W. Daehnick, M. J. Spisak, and J. R. Comfort, Phys. Rev. C 23, 1906 (1981).
[10]J. R. Comfort, Argonne National Laboratory Informal Report PHY-1970B, 1970 (unpublished).
[11]M. J. Martin, Nucl. Data Sheets (to be published); (private communication).
[12]T. T. S. Kuo and G. H. Herling, Naval Research Laboratory Report No. 2258, 1971 (unpublished); G. H. Herling and T. T. S. Kuo, Nucl. Phys. A181, 113 (1972).
[13]P. Richard, N. Stein, C. D. Kavaloski, and J. S. Lilley, Phys. Rev. 171, 1308 (1968); P. Mukherjee and B. L. Cohen, *ibid.* 127, 1284 (1962).
[14]Code CHUCK3 is the version of CHUCK2 written by P. D. Kunz, as extended by J. R. Comfort. CHUCK3 corresponds to the 1979 version of CHUCK2, in phase conventions (unpublished).
[15]W. W. Daehnick, J. D. Childs, and Z. Vrcelj, Phys. Rev. C 21, 2253 (1980).
[16]F. D. Becchetti and G. W. Greenless, in *Proceedings of the Third International Symposium on Polarization Phenomena in Nuclear Reactions, Madison, Wisconsin, 1970,* edited by H. H. Barschall and W. Haeberli (University of Wisconsin Press, Madison, Wisconsin, 1971), p. 682.
[17]J. R. Comfort, Comput. Phys. Commun. 16, 35 (1978).
[18]W. T. Pinkston and G. R. Satchler, Nucl. Phys. A383, 61 (1982).
[19]J. R. Comfort (private communication).
[20]J. R. Comfort and W. W. Daehnick (unpublished).
[21]M. A. Nagarajan and G. R. Satchler, Phys. Rev. Lett. 49, 1899 (1982).
[22]J. R. Comfort and W. W. Daehnick, Phys. Rev. Lett. 50, 1627 (1983).